



## An Autoregressive Integrated Moving Average (ARIMA) Based Forecasting of Ionospheric Total Electron Content at a low latitude Indian Location

Ram Kumar Vankadara<sup>(1)</sup>, Sudipta Sasmal<sup>(2)</sup>, Ajeet Kumar Maurya<sup>(3)</sup>, Sampad Kumar Panda\*<sup>(1)</sup>

(1) Department of ECE, Koneru Lakshmaiah Education Foundation, Vaddeswaram, AP, INDIA

(2) Institute of Astronomy Space and Earth Science, Salt Lake, Kolkata, INDIA

(3) Babasaheb Bhimrao Ambedkar University, Vidya Vihar, Raebareli Road, Lucknow, INDIA

Email: [sampadpanda@gmail.com](mailto:sampadpanda@gmail.com)

### Abstract

Ionospheric total electron content (TEC) plays an important role in introducing delay errors in space-based navigation and communication signals and requires early forecasting of the plausible impacts on the relying systems. In the present work, an autoregressive integrated moving average (ARIMA) is implemented in the time series analysis to forecast the TEC at an Indian low latitude location (KL University, Guntur; Geographic 16.37°N, 80.37°E) during the quiet (5-9 January 2021) and disturbed (3-7 March 2022) geomagnetic conditions. The performance of the model is evaluated from the biases, root mean square error (RMSE), and correlation coefficients between model forecast and observed TEC. The results show that bias remains between -3 to +3 TECU and +2 to -4 during quiet and disturbed days, respectively. The corresponding RMSE values are within a limit of 5 TECU and 6 TECU. The occurrence of plasma irregularities is also verified by analyzing the scintillation indices during the period. A further analysis refinement of the model is aimed to improve the forecasting accuracy over the region.

### 1. Introduction

The ionosphere plays a crucial role in space-based communication, navigation, and timing services as it introduces delays in the traversing signals. Total electron content (TEC) is a measurable quantity in the ionosphere that is corresponding to the characteristic ionospheric delays and is often considered for understanding the space weather influence on technological systems [1], [2]. The TEC is the total number of electrons encountered in the signal ray path from the satellite to the ground receiver, measured in electrons per square meter [3]. The rate of change of the TEC index (ROTI) is frequently used as a low-resolution proxy to the scintillation indices to define plasma irregularities [4]. Moreover, the high-resolution ionospheric TEC recorded by the specialized ionospheric monitoring Global navigation satellite system (GNSS) receivers is a good parameter to monitor the space weather effects and paves the possibility to develop time series data, and forecasting models. Time-series modeling is primarily concerned with gathering and analyzing available TEC

measurements to represent the underlying structures of TEC in the ionosphere. The daily, monthly, and seasonal variations of ionospheric TEC have been investigated earlier to evaluate the corresponding ionospheric delay [5]. Several time series models like Auto regression (AR), Moving Average (MA), Autoregressive moving average (ARMA), Autoregressive integrated moving average (ARIMA) models, and traditional models like International reference ionosphere (IRI), Ne-Quick models have been presented in the past for short term and long-term forecasting of ionospheric TEC [6]–[11]. The ionospheric delay is evaluated in terms of daily, monthly, and seasonal TEC variations using 3 forecasting models ARMA, ARIMA, and Holt-winters model. Erdoğan et al. [12] forecasted two days VTEC using the second order autoregressive (AR2) model. The observations gave 98% periodic and stochastic components and the 10-minute, 15-minute, and 20-minute forecasts gave good results. The long-term IGS data from 2006 to 2015 is used for analysis using the ARMA model. The prediction of VTEC showed that the precision is more in solar inactive years than the solar active years [13]. The comparative analysis of observed TEC with the IRI predicted values by Sharma et al. [14] at Manama, Bahrain suggests the model overestimates during daytime and underestimates at night.

In this paper, the forecasting performance of the ARIMA model is evaluated in a low latitude location where the input training data is obtained from continuously operating ionospheric TEC and scintillation monitoring specialized GNSS receiver, recently established at a low latitude location, KL University, Guntur, India. The TEC is forecasted for 5 days each in January (quiet condition) and March (disturbed condition) in 2022, using the ARIMA model. The efficiency of the forecast model is evaluated by analyzing the bias, RMSE, and correlation coefficients between the model and observed TEC values.

### 2. Data and Methodology

The TEC data used in this study are recorded by the multi-constellation and multi-frequency GNSS receiver (Septentrio/PolaRx5S) located at a low latitude station K L University campus (Geographic coordinates: 16.26°N,

80.37°E; Geomagnetic coordinates: 7.44°N, 153.75°E), Guntur, India. Figure 1 shows the geographic location of the receiver on the map along with the antenna/receiver setup. The technical details on this relatively newer GNSS receiver location are given in Vankadara et al. [15]. The system records the observations for a variety of GNSS constellations in ionospheric scintillation monitoring record (ISMR) format. The ISMR is a one-minute data that records the VTEC, amplitude scintillation index (S4 index), phase scintillation Index ( $\sigma\phi$  index), carrier to noise ratio, signal lock time for all the available signals and constellations recorded by the receiver.

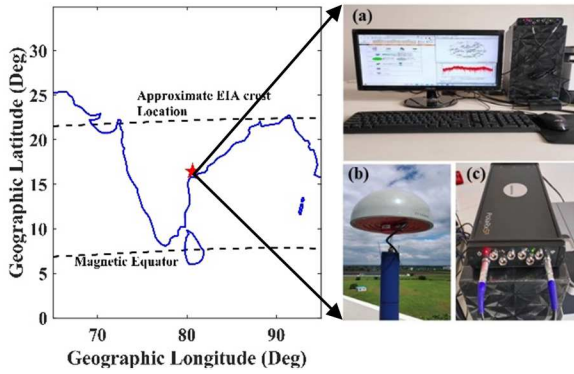


**Figure 1.** The location and the receiver setup used in this study. (a) Receiver Setup recording the data. (b) VeraChoke ring antenna. (c) PolaRx5S receiver.

The TEC corresponding to the legacy GPS L1 frequency is considered in this study as many of the single frequency applications are based on the aforesaid frequency. Autoregressive integrated moving average (ARIMA) models form a class of time series models that are widely applicable in the field of time series forecasting (Box et al., 2015). The ARIMA model is defined by the ARIMA (p, d, q) where p refers to the non-negative autoregressive term, d is the non-negative integrating term and q is the non-negative moving average term. The general form of the ARIMA (p, d, q) model is given by [16];

$$\phi_p(B)(1-B)^d X_t = c + \theta_q(B)\varepsilon_t \quad (1)$$

where p and q are non-negative orders of AR and MA processes, respectively;  $\phi_p$ ,  $\theta_q$  are coefficients of AR and MA components;  $X_t$  is the VTEC value at time t; d denotes the number of times data differenced; B is the backward shift operator where  $BV_t = V_{t-1}$ ; c is the constant term;  $\varepsilon_t$  is the error term whose normal distribution has zero mean and standard deviation ( $\sigma$ ). The lag order of the best ARIMA model is defined by the Autocorrelation function (ACF) and partial autocorrelation function (PACF) such that the maximum number of errors is minimized [17].

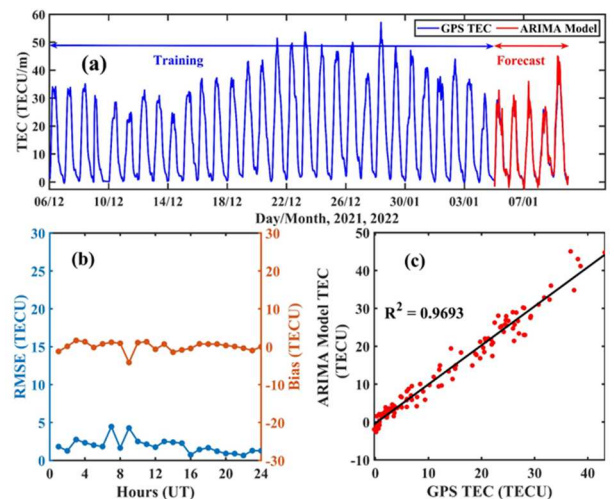
The TEC is forecasted for two cases: 5 days in January (DOY 3-7) and March (DOY 62-66) in the year 2022, corresponding to quiet and disturbed periods respectively. The disturbed and quiet days are chosen based on the list of international quiet days provided by the GFZ German Research Centre for Geosciences (<ftp://ftp.gfz->

<potsdam.de>). The elevation angle cut-off is taken at 40° to reduce the errors due to multipath and ground signal interference.

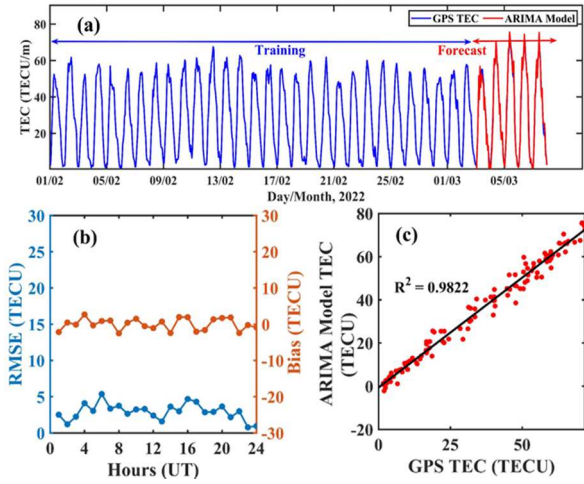
### 3. Results and Discussion

Figure 2 (a) depicts the variation of observed GPS TEC and the forecast TEC during the 5 days in January 2022. The blue color represents the observed TEC data which is taken for the training of the forecast model whereas the red color represents the forecasted TEC for March 3-7, 2022 which includes the geomagnetically disturbed days (March 5 and 6). The RMSE and bias error for the forecasted and observed data are given in Figure 2 (b). It can be observed from Figure 2 (c) that the forecast parameters are closely following the observed TEC during the disturbed geomagnetic condition with the correlation coefficient  $R^2=0.9822$ . The bias values are in a range of +3 to -3 TECU whilst the calculated RMSE values for the forecasted data range from 0 to 6 TECU.

Figure 3 (a) shows the forecasted TEC (in red color) during the quiet days and its comparison with the observed GPS TEC parameter. The training data (in blue color) is taken from December 2021 to forecast TEC for 5 days (3-7 January 2022). The RMSE and bias values between the forecast and observed TEC values are plotted in Figure 3 (b) and the maximum RMSE and range of biases are listed in Table 1. It is observed that the RMSE values for the forecasted period remain less than 5 TECU. The bias values of the forecasted data range from +2 to -4 units. The scatter plots between the observed TEC and forecasted TEC is shown in Figure 3 (c) wherein the coefficient of correlation is relatively high ( $R^2=0.9693$ ), referring to an excellent agreement between the forecast and observed TEC parameters.



**Figure 2.** The ionospheric VTEC forecasted from the ARIMA model for 5 to 9 January 2022. (a) shows the observed data (blue) for January and forecast data (red). (b) shows the RMSE and bias of the forecast data. (c) shows the correlation between the observed and forecast data.



**Figure 3.** The ionospheric VTEC forecasted from the ARIMA model for 3 to 7 March 2022. (a) shows the observed data (blue) for February and forecast data (red). (b) shows the RMSE and bias of the forecast data. (c) shows the correlation between the observed and forecast data.

**Table 1.** The mean RMSE, bias, and coefficient of correlation ( $R^2$ ) between the forecast TEC and observed TEC.

S. No	Month	Max. RMSE (in TECU)	Max. Bias (in TECU)	$R^2$
1	January-2022	6	3	0.9693
2	March-2022	5	2	0.9822

The maximum RMSE, maximum bias, and the correlation coefficient between the observed and modeled TEC are listed in Table 1. The results were produced in line with the previous studies on both quiet and disturbed days respectively [17]. To further understand the plasma irregularities during the forecast period, we analyzed the amplitude ( $S_4$ ) and phase ( $\sigma_\phi$ ) scintillation indices recorded by the specialized scintillation monitoring receiver (Septentrio/PolaRx5S). In Figure 4, the scintillation indices  $S_4$  and for the forecast days are shown both for the quiet days and disturbed days. Figure 4 (a) represents the  $S_4$  and  $\sigma_\phi$  indices for the 5-9 January ( quiet period) whereas Figure 4 (b) represents the  $S_4$  and  $\sigma_\phi$  indices for 3-7 March ( disturbed period). The  $S_4$  and  $\sigma_\phi$  during the selected disturbed period in March 2022 are very much higher than 5-9 January ( quiet period), inferring that the scintillations are predominantly occurring during the March equinox months. During the disturbed period, the  $S_4$  index reached up to 0.7, indicating moderate scintillation conditions whereas  $\sigma_\phi$  reached up to 0.2 with the magnitudes remaining within the ranges of weak scintillation conditions. The significant values for  $S_4$  and  $\sigma_\phi$  indices are observed in the post-sunset period in March. This corresponds to the occurrence of equatorial plasma bubbles (EPBs) during the local postsunset prereversal enhancement (PRE) sector [4] The postsunset EPBs

development over the equatorial and low latitude sector can be described through the Relay-Taylor instability originating from the bottomside of F-layer. During the quiet period, neither the  $S_4$  nor  $\sigma_\phi$  shows any significant values. Although the scintillation indices show increased magnitudes during the disturbed period, the forecast errors are minimum in March compared to January.

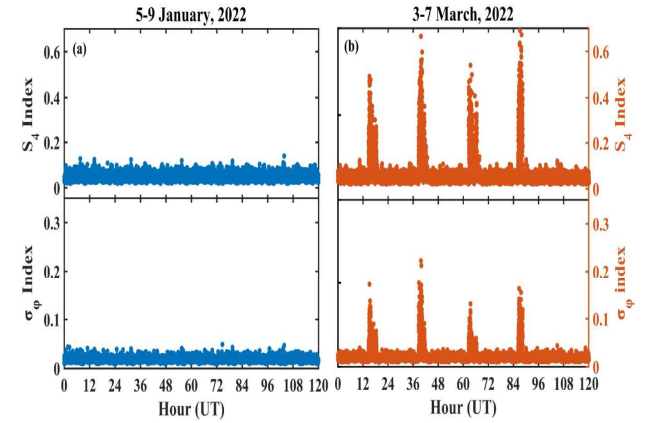


**Figure 4.** The observed  $S_4$  (blue) and  $\sigma_\phi$  (orange) for the 5 forecasted days for January and March 2022.

#### 4. Conclusion

In the present paper, the observed TEC and scintillation indices recorded by the newly established Septentrio/PolaRx5S ionospheric monitoring receiver at K L University campus in Guntur, India were considered in the analysis. The time series of TEC corresponding to GPS L1 frequency was used to train the ARIMA model for forecasting the parameter during both quiet (5-9 January 2022) and disturbed (3-7 March 2022) geomagnetic conditions. It is realized from the analysis that most of the time the forecast values are in line with the observed TEC values. The correlation coefficient between the forecast data and observed data is greater than 0.9 in both cases, indicating high linearity between both values. The maximum bias error between the observed TEC and forecast TEC is less than 5 TECU. The ARIMA model used only the lags from the previously trained data set and give the forecast values. It does not include the ionospheric dynamics during the forecast period. But these values can be used to alert the mitigation systems in case of any major disturbance observed through this model data. The model can be further refined by preprocessing the time-series data with the removal of possible noises. Further, consideration of long-term data from the newly established ionospheric monitoring receiver would enable improving the forecast accuracy of the model in future works.

#### 5. Acknowledgements

The quiet and disturbed days are taken from the list of international quiet days provided by the GFZ German Research Centre for Geosciences (<ftp://ftp.gfz->

[potsdam.de](http://potsdam.de)). The present work has been carried out under the Core Research Grant (CRG) project sponsored by the Science & Engineering Research Board (SERB) (A statutory body of the Department of Science & Technology, Government of India) in New Delhi, India, vide File No: CRG/2019/003394.

## 6. References

1. L. Liu, S. Zou, Y. Yao, and Z. Wang, "Forecasting Global Ionospheric TEC Using Deep Learning Approach," *Space Weather*, vol. 18, no. 11, p. e2020SW002501, Nov. 2020, doi: 10.1029/2020SW002501.
2. D. Sur and A. Paul, "Comparison of standard TEC models with a Neural Network based TEC model using multistation GPS TEC around the northern crest of Equatorial Ionization Anomaly in the Indian longitude sector during the low and moderate solar activity levels of the 24th solar cycle," *Advances in Space Research*, vol. 52, no. 5, pp. 810–820, Sep. 2013, doi: 10.1016/j.asr.2013.05.020.
3. S. S. K. Rajana, T. S. Shrungheshwara, C. G. Vivek, S. K. Panda, and S. Jade, "Evaluation of long-term variability of ionospheric total electron content from IRI-2016 model over the Indian sub-continent with a latitudinal chain of dual-frequency geodetic GPS observations during 2002 to 2019," *Adv. Space Res.*, vol. 69, no. 5, pp. 2111–2125, 2022, doi: 10.1016/j.asr.2021.12.005.
4. R. K. Vankadara *et al.*, "Signatures of Equatorial Plasma Bubbles and Ionospheric Scintillations from Magnetometer and GNSS Observations in the Indian Longitudes during the Space Weather Events of Early September 2017," *Remote Sens.*, vol. 14, no. 3, 2022, doi: 10.3390/rs14030652.
5. G. Sivavaraprasad and D. V. Ratnam, "Performance evaluation of ionospheric time delay forecasting models using GPS observations at a low-latitude station," *Advances in Space Research*, vol. 60, no. 2, pp. 475–490, 2017.
6. K. Ansari, S. K. Panda, O. F. Althuwaynee, and O. Corumluoglu, "Ionospheric TEC from the Turkish Permanent GNSS Network (TPGN) and comparison with ARMA and IRI models," *Astrophysics and Space Science*, vol. 362, no. 9, p. 178, Aug. 2017, doi: 10.1007/s10509-017-3159-z.
7. I. Srivani, G. Siva Vara Prasad, and D. Venkata Ratnam, "A Deep Learning-Based Approach to Forecast Ionospheric Delays for GPS Signals," *IEEE Geoscience and Remote Sensing Letters*, vol. 16, no. 8, pp. 1180–1184, 2019, doi: 10.1109/LGRS.2019.2895112.
8. M. Kaselimi, A. Voulodimos, N. Doulamis, A. Doulamis, and D. Delikaraoglou, "A Causal Long Short-Term Memory Sequence to Sequence Model for TEC Prediction Using GNSS Observations," *Remote Sensing*, vol. 12, no. 9, 2020, doi: 10.3390/rs12091354.
9. W. Sun *et al.*, "Forecasting of ionospheric vertical total electron content (TEC) using LSTM networks," in *2017 International Conference on Machine Learning and Cybernetics (ICMLC)*, Jul. 2017, vol. 2, pp. 340–344. doi: 10.1109/ICMLC.2017.8108945.
10. S. Kumar, K. Patel, and A. K. Singh, "TEC variation over an equatorial and anomaly crest region in India during 2012 and 2013," *GPS Solutions*, vol. 20, no. 4, pp. 617–626, Oct. 2016, doi: 10.1007/s10291-015-0470-4.
11. D. V. Ratnam, Y. Otsuka, G. Sivavaraprasad, and J. R. K. K. Dabbakuti, "Development of multivariate ionospheric TEC forecasting algorithm using linear time series model and ARMA over low-latitude GNSS station," *Advances in Space Research*, vol. 63, no. 9, pp. 2848–2856, 2019, doi: <https://doi.org/10.1016/j.asr.2018.03.024>.
12. H. Erdoğan and N. Arslan, "Identification of vertical total electron content by time series analysis," *Digital Signal Processing*, vol. 19, no. 4, pp. 740–749, Jul. 2009, doi: 10.1016/j.dsp.2008.07.002.
13. Y. Kong, H. Chai, J. Li, Z. Pan, and Y. Chong, "A modified forecast method of ionosphere VTEC series based on ARMA model," in *2017 Forum on Cooperative Positioning and Service (CPGPS)*, May 2017, pp. 90–95. doi: 10.1109/CPGPS.2017.8075103.
14. S. K. Sharma, K. Ansari, and S. K. Panda, "Analysis of Ionospheric TEC Variation over Manama, Bahrain, and Comparison with IRI-2012 and IRI-2016 Models," *Arab. J. Sci. Eng.*, vol. 43, no. 7, pp. 3823–3830, 2018, doi: 10.1007/s13369-018-3128-z.
15. R. K. Vankadara, K. D. Reddybattula, and S. K. Panda, "Multi-constellation GNSS Ionospheric Scintillation Monitoring through PolaRx5S Receiver at a low latitude station in India," in *2021 IEEE International Women in Engineering (WIE) Conference on Electrical and Computer Engineering (WIECON-ECE)*, Dec. 2021, pp. 184–187. doi: 10.1109/WIECON-ECE54711.2021.9829648.
16. G. E. Box, G. M. Jenkins, G. C. Reinsel, and G. M. Ljung, *Time series analysis: forecasting and control*. John Wiley & Sons, 2015.
17. X. Zhang, X. Ren, F. Wu, and Q. Lu, "Short-term TEC prediction of ionosphere based on ARIMA model," *Acta Geodaetica et Cartographica Sinica*, vol. 43, no. 2, pp. 118–124, 2014, doi: 10.13485/j.cnki.11-2089.2014.0018.